Fundamental Research 5 (2025) 516–525

Contents lists available at ScienceDirect

Fundamental Research

journal homepage: http://www.keaipublishing.com/en/journals/fundamental-research/

Review

Coherent detection of pulsed terahertz waves in solid, gaseous, and liquid media

Guoyang Wang[a,1], Ruoxi Wu[a,1], Liangliang Zhang[a,*], Cunlin Zhang[a], X.-C. Zhang[b,*]

[a] Department of Physics, Key Laboratory of Terahertz Optoelectronics (MoE), Capital Normal University, Beijing 100048, China
[b] The Institute of Optics, University of Rochester, Rochester, NY 14627, USA

ARTICLE INFO

Article history:
Received 26 July 2024
Received in revised form 5 August 2024
Accepted 18 August 2024
Available online 24 August 2024

Keywords:
Terahertz wave
Coherent detection
Photoconductive antenna
Electro-optic sampling
Gas plasma
Free-flowing liquid

ABSTRACT

Coherent detection measures both the amplitude and phase of pulsed terahertz (THz) waves simultaneously, forming the foundation for THz time-domain spectroscopy (THz-TDS). This technique has become increasingly prominent in the fields of physics and materials science, allowing researchers to investigate the dynamic properties of various dielectric materials within the 0.1 to 10 THz frequency range, which is previously a challenging spectrum to access. This paper reviews recent advancements and the challenges faced by commonly used coherent detectors in THz-TDS. Our discussion emphasizes the potential for new discoveries in THz photonics and highlights the crucial role of coherent detection in the study of laser-matter interactions.

1. Introduction

The terahertz (THz) frequency ranges from 0.1 to 10 THz and is located between millimeter and infrared waves (see Fig. 1), which is one of the most elusive regions of the electromagnetic spectrum [1-5]. Due to its longer wavelength compared to optical or infrared radiation, many dielectric materials that appear opaque at shorter wavelengths due to scattering effects are transparent in the THz range. This transparency allows for the non-destructive examination of their internal macroscopic structures [6,7]. Additionally, some molecules exhibit absorption at specific resonance frequencies due to vibrational and rotational activities, enabling a detailed understanding of their microscopic dynamics and identification through their unique THz signatures [8,9]. These characteristics make THz technology highly attractive for a variety of practical applications as well as fundamental studies in physics, chemistry, and biology.

Significant progress of applying THz waves to realize non-invasive technology has been made in the biomedical field, because of the low energy of THz photons (4 meV at 1 THz) and the alignment of covering most biomolecular vibrational and rotational frequencies [10-12]. Chang's group firstly observed that the myelin sheath can serve as an infrared to THz waveguide, promoting the label-free detection of biological tissues due to the ability of deep penetration through the myelin [13]. THz stimulus can serve as an efficient, nonthermal, and long-range method to accelerate the unwinding process of DNA duplexes, which is the basis of gene duplication and editing [14]. Moreover, they further clarified that the resonant THz field could manipulate the conduction of calcium channels, which has potential applications in therapeutic intervention [15]. It is prospective that THz waves activate brain neurons and induce firing activities in vivo without introducing any exogeneous gene [16]. These advancements have propelled THz research to new heights and expanded its application prospects significantly.

Over the past two decades, there has been a revolution in THz time-domain spectroscopy (THz-TDS) systems, driven by the development of high power sources. These demonstrated the potential of THz technology for fundamental research and commercial application. In contrast to conventional optical spectroscopy methods that measure light intensity at specific frequencies, THz-TDS measures the electric field of THz pulses over time. By applying Fourier transform of the recorded time-domain signal, researchers can obtain both the amplitude and phase of the THz pulse, enabling precise measurements of the absorption coefficient and refractive index of materials interacting with THz waves

* Corresponding authors.
E-mail addresses: liangliang_zhang@cnu.edu.cn (L. Zhang), xi-cheng.zhang@rochester.edu (X.-C. Zhang).
[1] These authors contributed equally to this work.

https://doi.org/10.1016/j.fmre.2024.08.003

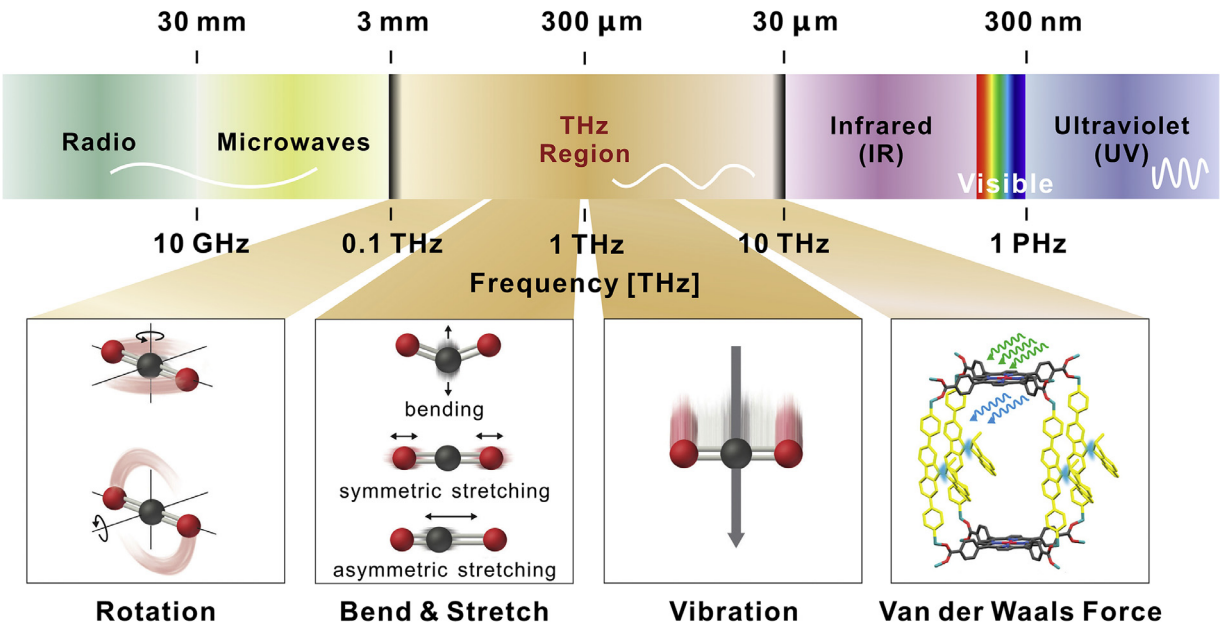

Fig. 1. Electromagnetic spectrum. The THz frequency band bridges the gap between millimeter wave and infrared wave, and it corresponds to molecular phenomena such as rotation, bending and stretching, vibration, and interaction influenced by Van der Waals force.

[17]. Existing THz sources such as photoconductive antenna (PCA), optical rectification, and air plasma could generate intense (260 MV/cm) [18] and broadband (100 THz) [19] THz pulses. High-order and high-sensitivity detectors are essential for improving detection accuracy and sensitivity. Consequently, the development of superior detection technologies and enhancement of detection performance are crucial issues to address.

This review focuses on the coherent detection of pulsed THz waves using solid, gaseous, and liquid materials, as shown in Fig. 2. Section 2 introduces solid-based approaches, including PCA and electro-optic sampling (EOS), which contribute to high detection sensitivity. The following section discusses coherent detection based on air plasma, extending to omnidirectional detection through THz radiation-enhanced emission of fluorescence and acoustics. Finally, recent advancements in THz wave detection using free-flowing liquids, such as water and related materials, are described. We examine the state-of-the-art development and application of detection techniques based on the requirements of THz science and technology.

2. Highly sensitive detection using solid materials

Semiconductors with high carrier mobilities and crystals with high electro-optic (EO) coefficients are exemplary solid materials for detecting THz waves. The coherent detection of THz pulses was first achieved by PCA in 1988 [20], enabling the recording of THz time-domain waveforms. In 1995, EOS was proposed to offer a more feasible and stable detection method [21]. THz signals detected by solid materials typically exhibit high sensitivities and signal-to-noise ratios (SNRs), making them the most common detectors for THz waves.

2.1. Photoconductive antenna

A PCA typically consists of a semiconductor substrate and two electrodes separated by a gap. Detection of THz waves using a PCA is essentially the reverse process of THz emission from a PCA. When femtosecond laser pulses irradiate the gap, they excite charge carriers into the conduction band. The THz electric field then accelerates these charge carriers, generating a transient photocurrent [22]. This induced current $I(t)$ is proportional to the input THz electric field $E_{THz}(t)$:

$$I(t) = \int_{-\infty}^{t} \sigma_s(t-t')E_{THz}(t')dt' \quad (1)$$

where σ_s denotes the transient surface conductivity. By adjusting the relative time delay between the THz and optical pulses, the time-domain waveform of THz pulses can be acquired by measuring the current variation over time. The signal is measured using a lock-in amplifier after passing through an optical chopper.

To increase the detection bandwidth, it is preferable to use substrate materials with shorter carrier lifetimes, such as low-temperature or doped gallium arsenide (GaAs), along with optical laser pulses of shorter durations. For instance, a PCA with doped GaAs and 15 fs optical laser pulses can detect THz frequencies up to 30 THz [23-25]. The bandwidth can be extended to 100 THz using PCA with low-temperature GaAs and a 10 fs optical laser. The geometry of the electrodes also impacts the bandwidth [19]. There are four main geometric shapes: strip lines [26], bow ties [27], butterflies [28], and logarithmic antennas [29]. Butterfly-shaped PCAs are commonly used for detecting low-frequency THz pulses, while strip lines are more sensitive to high frequencies. Additionally, a narrower gap allows for the detection of higher frequencies, and longer electrodes can increase the amplitude of the detected signal.

Recent advancements have further improved PCA detector performance through surface plasmon and nanotechnology related methods. Techniques such as manipulating large-area plasma gratings, THz concentrators, optical nanoantenna arrays, and plasma nanocavities have been adopted [30-33]. For example, using a plasma nanocavity, all photocarriers are generated within 100 nm of the photoconductive contact electrode, resulting in minimal transmission time for almost all photogenerated carriers. This approach has yielded detectors with a SNR of 100 dB and a noise-equivalent bandwidth of 0.1–6 THz [34].

Due to the high sensitivity and stability of PCA detectors, many companies now offer PCAs with exceptional performance. For instance, the Interdigital array antenna (iPCA-21–05–10–800-x) from the German company Batop can achieve a detection bandwidth of 0.1–4.5 THz under 800 nm laser excitation. Similarly, the Bow tie antenna (bPCA-3000–05–10–1550-x) can achieve the same detection bandwidth under 1550 nm laser excitation. Menlo Systems' fiber-coupled antenna module

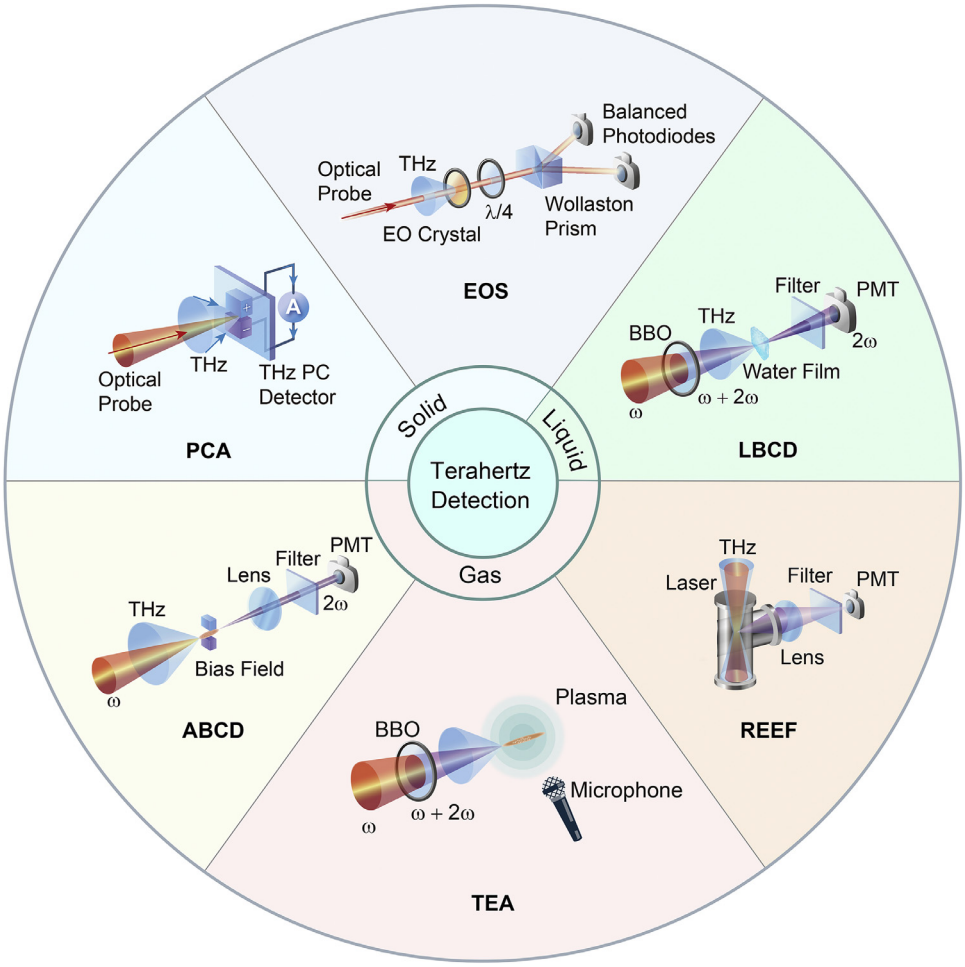

Fig. 2. Coherent detection schemes of THz waves based on solids, gases and liquids. PCA, Photoconductive antenna; EOS, Electro-optic sampling; ABCD, Air-biased coherent detection; TEA, THz-enhanced acoustics; REEF, Radiation-enhanced fluorescence emission; LBCD, Liquid-based coherent detection.

(TERA15-RX-FC) is suitable for 1560 nm laser excitation, offering a detection bandwidth greater than 6 THz. These PCAs are compact enough to be utilized in THz-TDS.

2.2. Electro-optic sampling

A second-order nonlinear crystal can also be used to detect THz waves through EOS [35,36]. In this process, the THz field induces birefringence in the crystal via the Pockels effect, which is the linear dependence of the refractive index on the electric field of the incident radiation. A linearly polarized femtosecond laser passes through an EO crystal and then through a quarter-wave plate, changing the polarization to circular. A Wollaston prism separates the orthogonal polarization components of the laser, which are then detected separately by two photodiodes. The output signal is the difference between them. Without a THz pulse, the optical laser remains circularly polarized, resulting in no difference in the photodiode signals ($I = 0$). However, when an optical probe pulse co-propagates with a THz pulse through the crystal, the THz-field-induced birefringence alters the ellipticity of the probe pulse. The difference (I) in the photodiode signals directly provides the amplitude of the THz electric field using the following formula:

$$I = I_y - I_x = I_0 \Delta\phi \propto E_{THz}, \tag{2}$$

$$I_x = I_0(1 - \sin\Delta\phi)/2 \approx I_0(1 - \Delta\phi)/2, \tag{3}$$

$$I_y = I_0(1 + \sin\Delta\phi)/2 \approx I_0(1 + \Delta\phi)/2. \tag{4}$$

where I_0 is the total intensity of the detection beam, and $\Delta\phi$ is the phase delay between the two polarization components. By scanning the time delay between the femtosecond laser and the THz pulse, the entire THz waveform can be recorded.

Phase matching between the optical laser and the THz wave in the EO crystal is crucial for effective EOS. For example, ZnTe crystals are commonly used for THz wave detection with optical lasers at a wavelength of 800 nm. In the noncollinear extension of the ellipsometric technique, the optical laser propagates through the EO crystal at a Cherenkov angle to the THz beam [37,38]. This configuration allows for synchronous propagation of THz waves and optical lasers of any wavelength in crystals, eliminating phase mismatch. The non-ellipsometric scheme operates by spatially separating the sum-frequency generation and difference-frequency generation (DFG) contributions of opposite polarities to the optical intensity modulation.

Birefringent crystals that meet the phase-matching conditions for DFG, such as isotropic crystals (e.g., ZnTe, GaAs, GaP), are suitable for low-frequency THz wave detection. Conversely, certain anisotropic crystals (e.g., GaSe, $AgGaS_2$, $LiGaS_2$) can coherently detect high-frequency THz waves through second-order nonlinear processes [39-42]. Additionally, organic crystals such as 4-N, N-dimethylamino-4′-N′-methylhexenestramonium 2,4,6-trimethylbenzenesulfonate (DSTMS) and diphenylfluoroketone (DPFO) are suitable for EOS with a bandwidth covering the entire THz frequency range [43,44]. Furthermore, detection efficiency can be improved by cooling the crystal [45-48]. Cooling ZnTe crystals from 300 K to 1.5 K enhances detection sensitivity by more than an order of magnitude [49]. Theoretical calculations attribute this

Table 1
Parameters of common EO crystals.

Crystal	EO coefficient (pm/V) / λ (nm)	n_{Laser}	n_{THz} / f (THz)	α_{THz} (cm^{-1}) / f (THz)	Bandwidth (THz) / Thickness (mm)
ZnTe [35]	4/800	2.85	3.17/1.6	1.3/1.6	0.2–4/1
GaP [36]	1/800	3.67	3.34/2	0.2/2	0.1–7/0.15
$LiNbO_3$ [50,51]	28/800	2.25	4.98/1	18.2/1	0.1–2.5/2
DSTMS [52,53]	49/1500	2.19	2.2/5	20/5	0.1–20/0.73
DAST [52,53]	47/1500	2.26	2.3/5	30/5	0.1–20/0.54

significant enhancement to the reduction in THz wave absorption and phase-matching variations as the temperature decreases.

Table 1 lists common EO crystals and their corresponding parameters. ZnTe is the most widely used detection crystal due to its excellent phase-matching conditions, although it has a relatively narrow bandwidth [35]. GaP crystals offer a broader response, requiring a very thin layer to avoid phase mismatch between the optical laser and the THz wave [36]. $LiNbO_3$ has a high damage threshold and is highly transparent to 800 nm lasers [50,51], but it suffers from a substantial mismatch between the group velocity of the optical laser and the phase velocity of the THz wave, necessitating the use of noncollinear ellipsometric techniques. Organic crystals exhibit the broadest bandwidths but have a low damage threshold and are only suitable for use with 1500 nm wavelength lasers [52,53]. The detection sensitivity and bandwidth are influenced by several factors, including the thickness and quality of the crystal, as well as the wavelength and pulse duration of the optical laser.

While PCA and EOS are common methods for detecting THz waves using solid materials, their bandwidths are limited by the carrier lifetime in semiconducting photoconductors and phonon absorption in EO crystals. Additionally, the low damage threshold of semiconductor materials can lead to nonlinear effects in the semiconductor substrates under strong THz fields, complicating the acquisition of accurate detection signals. Recent studies have shown that focusing a strong THz wave (260 MV/cm) on a semiconductor can cause tunneling ionization [18]. Consequently, high-damage-threshold materials, such as those based on graphene and perovskites, are being explored for the development of THz antennas [54,55]. EOS is not suitable for detecting intense THz fields if the polarization rotation angle exceeds $\pi/2$, as this causes signal reversal (over-rotation) [56]. To prevent this, the THz pulse energy must be reduced using additional THz polarizers or multiple silicon plates, which can lead to inaccurate measurements [57]. The low damage threshold of solid materials makes them prone to ionization breakdown by optical lasers. This issue remains unresolved, prompting the development of THz wave detection technologies based on gas and liquid media.

3. Ultra-broadband and remote sensing based on gaseous medium

Gases are excellent candidates for THz sensors due to their unique properties: the absence of phonons and dispersion, no damage threshold, and continuous regenerative capabilities. These qualities enable the detection of THz pulses with ultrabroad bandwidths covering the entire THz spectrum. Through the third-order nonlinearity present in all gases, three photons—two from the laser beam and one from the THz pulse—can interact to produce a photon near the second harmonic of the laser frequency. The THz field can be detected through measuring the induced second harmonic. Care must be taken to ensure measurements provide both the amplitude and phase of the second harmonic pulse. Additionally, two indirect detection methods including THz radiation-enhanced fluorescence emission (THz-REEF) and THz-enhanced acoustics (TEA) have been employed to detect THz waves by measuring the fluorescence and acoustic emission from laser-induced air plasma. These techniques enable the coherent detection of THz waves by "seeing" the fluorescence or "hearing" the acoustics of the plasma. They offer omnidirectional optical signal collection and are not limited by the absorption of THz waves by water vapor in ambient air, thereby enabling long-distance THz wave sensing.

3.1. Coherent detection through the third order nonlinearity of gases

Similar to the generation of THz waves in a centrosymmetric medium, which requires an odd number of input photons, the detection of THz waves in gas media also adheres to these symmetry requirements [58]. THz-wave detection in gases is accomplished through a four-wave mixing process, where two input photons are at the fundamental laser frequency and one is a THz photon. The emitted second harmonic field is proportional to the product of the three input fields, as expressed below [59]:

$$E_{2\omega}^{signal} \propto \chi^{(3)} E_{\omega} E_{\omega} E_{THz} \tag{5}$$

where $\chi^{(3)}$ is the third-order nonlinear coefficient of air plasma, E_{ω} represents the electric field of the fundamental frequency laser. The THz field-induced second harmonics (TFISH) are detected using a photomultiplier tube (PMT). During measurement, the power of the second harmonic is measured [58].

$$I_{2\omega} \propto \left|E_{2\omega}\right|^2 \propto \left(\chi^{(3)} I_{\omega}\right)^2 E_{THz}^2 \tag{6}$$

Consequently, this measured quantity is proportional to the intensity, which is proportional to the square of the THz electric field, resulting in incoherent detection. However, when THz waves are measured in gases, there is a background second-harmonic signal from the white light emitted by the air plasma, designated as $E_{2\omega}^{LO}$, resulting in homodyne detection of the THz field. The resulting second harmonic intensity then becomes [59]:

$$\begin{aligned} I_{2\omega} \propto \left(E_{2\omega}\right)^2 &= \left(E_{2\omega}^{signal} + E_{2\omega}^{LO}\right)^2 \\ &= \left(E_{2\omega}^{signal}\right)^2 + \left(E_{2\omega}^{LO}\right)^2 + 2E_{2\omega}^{signal} E_{2\omega}^{LO} \cos(\varphi) \end{aligned} \tag{7}$$

which includes a cross-term with a linear dependence on the THz field. If $E_{2\omega}^{LO}$ is much larger than the field of TFISH, the cross-term dominates, resulting in quasi-coherent detection of the THz waves. The homodyne technique partially addresses the challenge of coherent THz wave detection using a four-wave mixing process. However, it has notable disadvantages: it remains coherent only within a specific range of THz field values and can distort the waveform if the field is too high. Furthermore, the requirement for $E_{2\omega}^{LO}$, to be significantly larger than the signal necessitates a large background signal, complicating the achievement of an adequate dynamic range for THz-TDS.

To overcome these limitations, employing a heterodyne technique can lift the intrinsic limit on THz field strength and ensure coherent detection [60]. Similar to TFISH generation, a second-harmonic signal can be produced using a DC electric field as one of the inputs, in a method known as air-biased coherent detection (ABCD). Assuming the nonlinear susceptibility of the two processes is the same and that they are plane waves, the following expression is obtained [58]:

$$E_{2\omega} \propto \chi^{(3)} E_{\omega} E_{\omega} \left(E_{THz} + E_{DC}\right) \tag{8}$$

which again contains a coherent cross-term in the expression for the second-harmonic intensity:

$$I_{2\omega} \propto \left|E_{2\omega}\right|^2 \propto \left(\chi^{(3)} I_{\omega}\right)^2 \left(E_{THz}^2 + 2E_{THz} E_{DC} + E_{DC}^2\right) \tag{9}$$

In contrast to the second-harmonic generation using a white light local oscillator, the phase of the DC field-induced second harmonic can be readily controlled. Simply altering the direction of the electric field results in a π shift in the carrier phase of the second harmonic pulse. This modification changes the sign of the cross-term while leaving the other terms unaffected [61]. Therefore, by using an AC field synchronized with laser pulse repetition, the cross-term is modulated at the AC frequency. In the ABCD method, employing a modulated bias induces a heterodyne process that isolates only the coherent term of the measurement. This approach does not require matching the relative amplitudes of the THz and bias fields, thus allowing the measurement of a large THz field against a minimal background and enhancing the potential dynamic range. The detection bandwidth can be expanded by shortening the laser pulse duration [60]. For example, with a 120 fs laser pulse, the bandwidth encompasses up to 10 THz. However, compressing the pulse to 32 and 10 fs extends the bandwidth to 40 THz [62] and 200 THz [63], respectively.

The sensitivity of the ABCD technique can be increased through a balanced heterodyne detection scheme, which employs a polarization-dependent geometry. By exploiting the tensor properties of third-order nonlinear susceptibility, second-harmonic pulses with two orthogonal polarizations were detected by two separated PMTs. The outputs from the PMTs were subtracted using a balanced detection circuit, which mitigates the noise from laser fluctuations, thereby doubling the SNR [64,65]. Another effective strategy for enhancing the sensitivity of gas plasma detection involves selecting gases with high nonlinear properties, appropriate gas pressures, and optimized detection pulse energies [66-68]. Experimental studies have shown that nonlinear gases such as N_2, Xe, SF_6, CS_2, C_5H_8, and various alkanes are particularly effective in detecting THz waves. Notably, propane has demonstrated a detection signal strength 40 times greater than that of air under comparable conditions [66,67]. Additionally, the unipolar polarization method in THz wave detection allows for direct measurement of both the amplitude and polarization angle of the THz field in the time domain [61,69-71].

By integrating β-BBO crystals into the optical pathway, TFISH along with a controlled second harmonic facilitates broadband THz wave coherence detection, termed optically biased coherent detection (OBCD) [72]. This method affords precise control over the intensity, phase, and polarization of frequency-doubled laser light. By adjusting the bias of the second harmonics, which are absent in the supercontinuum, the phase difference can be manipulated using dispersion optics to achieve heightened sensitivity. The OBCD method is capable of resolving the orthogonal polarization components of the THz field and enables the measurement of THz wave polarization by rotating the polarization of the fundamental laser [73].

Although gas plasma-based coherent detection methods offer broadband capabilities, they are unable to capture TFISH signals from backward or lateral directions. Furthermore, the strong attenuation of water vapor at THz frequencies restricts the propagation distance of broadband THz pulses [74], rendering these methods unsuitable for long-distance coherent detection.

3.2. THz radiation-enhanced emission of fluorescence

When a gas is exposed to a strong laser pulse, photoionization liberates free electrons from the atoms or molecules, and the absorption of multiple optical photons creates many higher energy states. These states are nearly at the ionization threshold, making them highly susceptible to further ionization by collisions with nearby high-energy electrons, which then produce fluorescence [75-77]. In ambient air, nitrogen molecules are the primary source of fluorescence in the ultraviolet spectrum, with wavelengths ranging from 300 to 500 nm. Upon illumination by a THz pulse, the plasma's free electrons gain kinetic energy, leading to further ionization of the molecule through collisional interactions. This process significantly enhances fluorescence emissions from the molecules or ions [78-81]. The time derivative of the enhanced fluorescence is proportional to the square of the THz field, exhibiting a constant phase delay. This characteristic facilitates incoherent THz wave detection with a temporal resolution defined by the ionizing pulse envelope. Additionally, coherent detection employing THz-REEF is feasible when an external bias, aligned parallel to the THz field, is applied to the plasma acting as a local oscillator [75].

In a setup utilizing synthetic light fields from two-color pulses, ionized electrons acquire an asymmetric drift velocity. The polarization and relative phase of the two laser fields are critical in manipulating the drift velocity distribution and, consequently, the electron trajectory. The amplitude and direction of the THz field directly affect the plasma fluorescence, with the THz waveform information being encoded through the observed changes in fluorescence caused by different time delays between the THz pulse and laser pulses. By measuring the time-dependent fluorescence emission, one can accurately characterize THz waveforms. The total enhanced fluorescence emission, denoted as *FL*, resulting from energy transfer over an extended duration, can be expressed as [79]:

$$\Delta I_{FL}\left(\Delta\varphi_{\omega,2\omega}\right) \propto n_e\left[\int_{-\infty}^{+\infty}\left(m_e v^2(0)+2m_e v(0)\Delta v_1\right)\times\rho\left(v(0),\Delta\varphi_{\omega,2\omega}\right)dv(0)/2+\left(m_e\sum_{i=1}^{\infty}\Delta v_i^2\right)\right] \tag{10}$$

where $\Delta v_i=-\int_{t_i-\tau}^{t_i} eE_{THz}(t)dt/m_e$, τ is the electron relaxation time, n_e denotes the electron density, and $m_e v^2(0)$ term corresponds to the energy transferred by the initial electron kinetic energy from the laser intensity. The first-order term, $2m_e v(0)\Delta v_1$, is attributed to the acceleration before the initial impact, while the second-order term, $m_e\sum_{i=1}^{\infty}\Delta v_i^2$, represents the energy imparted from the external THz field. Given that the electron relaxation time is significantly shorter than the period of the THz pulse, the THz field can be approximated as nearly constant between adjacent collisions. By calculating the difference between $\Delta I_{FL}(\Delta\varphi_{\omega,2\omega}=\pi/2)$ and $\Delta I_{FL}(\Delta\varphi_{\omega,2\omega}=-\pi/2)$, insights into the time-dependent THz field can be directly obtained:

$$\Delta I_{FL}\left(\Delta\varphi_{\omega,2\omega}=-\pi/2\right)-\Delta I_{FL}\left(\Delta\varphi_{\omega,2\omega}=\pi/2\right)\propto n_e\rho\left(v_e,0\right)e\tau v_e(0)E_{THz}\propto E_{THz} \tag{11}$$

The fluorescence emission from the two-color laser plasma was observed to be 50% greater than that from the non-overlapping pulses. This method is unaffected by multiple reflections of THz pulses at the detector-air interface, thereby eliminating any limitations on the time window of the signal. THz-REEF effectively mitigates the issue of atmospheric moisture absorbing THz waves. By capturing time-resolved THz-REEF, the temporal waveform of the THz field can be determined from the transient enhanced fluorescence, making THz-TDS valuable for omnidirectional and coherent detection [82]. Although the fluorescence collection efficiency diminishes with increasing distance and the SNR of the THz wave decreases, the system can still accurately reproduce the THz waveform at various distances and distinctly identify the THz spectrum up to a distance of 10 m, thus facilitating long-distance detection [79]. However, THz-REEF does have some limitations. Firstly, the resolution is constrained by the scattering frequency of electrons in the plasma. For frequency components significantly higher than this scattering frequency, the sensitivity of this detection method decreases compared to that of the lower-frequency components. Secondly, the fluorescence cannot penetrate obstacles that are opaque to visible light. Lastly, there is a safety concern with the use of strong amplifier lasers, which pose potential risks to human eyesight.

3.3. THz radiation-enhanced acoustics

TEA utilizes laser plasma photoacoustics for the detection of THz waves. Under the irradiation of powerful femtosecond laser pulses,

molecules undergo photoionization on a sub-picosecond timescale. The laser field heats the free electrons, while the neighboring molecules or ions remain substantially cooler. As these hot electrons collide with surrounding air molecules, energy is transferred, gradually leading to thermal equilibrium. This process results in the translational motion of the molecules, generating a shock wave that transforms into sound waves [83]. When a laser pulse spatially overlaps and precedes the THz pulse, the THz field amplifies the sound pressure [84,85]. This acoustic emission from single-color laser-induced plasma is an effective means to detect THz waves [86]. The benefits of this detection method include: a) its omnidirectional mode, where signals are collected from any direction, and b) its robustness against water vapor interference, which is particularly advantageous for long-distance detection. However, a limitation of this method is its inability to capture the phase information of the THz pulse from the acoustic signal.

To investigate the influence of the optical phase on the velocity distribution of electron drift, a second-harmonic laser field was introduced to isolate the energy absorbed by the electrons from the THz field before their collision. This approach facilitated a physical understanding of how the dual-frequency field affects the path of free electrons in plasma, translating THz spectral information into sound waves. In the acoustic emission of a two-color laser-induced air plasma, the enhancement of the sound pressure can be expressed as follows [84]:

$$\Delta p\left(\Delta\phi_{\omega,2\omega}\right) \propto n_e \left[\int_{-\infty}^{+\infty} \left(m_e \vec{v}^2(0) + 2 m_e \vec{v}(0) \Delta \vec{v}_{e1} \right) \times \rho\left(\vec{v}(0), \Delta\phi_{\omega,2\omega}\right) d\vec{v}(0)/2 + m_e \sum_{i=1}^{\infty} \Delta \vec{v}_{ei}^2 \right] \tag{12}$$

where $\Delta\vec{v}_{ei}$ represents the effect of the change in the THz field on the electron velocity during two consecutive electron-molecule collisions, and $\phi_{\omega,2\omega}$ indicates the relative phase between the two laser fields. Given that the electron relaxation time τ is shorter than the duration of the THz pulse under atmospheric pressure, the pressure increase (Δp) can be approximated as $e^2\tau \int_{t_D}^{\infty} E_{THz}(t')^2 dt'/m_e$.

Owing to the relationship $\Delta v_{ei} = -\int_{t_i-\tau}^{t_i} eE_{THz}(t)dt/m_e$, the direct correlation between the THz electric field strength and the increase in sound pressure can be explicitly defined as:

$$\Delta p(\pi/2) - \Delta p(-\pi/2) \propto \vec{E}_{THz} \tag{13}$$

Therefore, TEA from plasma induced by two-color laser fields offers a unique solution for coherent THz wave detection. An acoustic enhancement of approximately 10% is observed across the 140 kHz bandwidth of the broadband microphone signal when using 100 μJ pulse energy at a wavelength of 800 nm for the laser pulses [84,86]. In both scenarios, the THz-field-induced heating of electrons and the subsequent increase in electron-electron, electron-ion, and electron-molecule collisions lead to enhanced acoustic waves. A detailed study of laser-induced photoacoustics reveals a unique method for remotely and omnidirectionally detecting THz waves by "listening" to the interaction of laser-induced plasma with pulsed electromagnetic radiation.

While both THz-REEF and TEA can achieve long-distance omnidirectional THz wave detection, the acoustic pressure decreases with radial distance at rate $1/r$ and fluorescence signal decreases with $1/r^2$. A THz system utilizing gas photonics for both generation and detection boasts unique features, such as a broad, continuous bandwidth that spans the entire THz range. Various geometries have been introduced to optimize the efficient use of input laser energy, as well as the dynamic range and bandwidth. However, significantly improving detection sensitivity remains challenging due to the low molecular density of the gaseous medium.

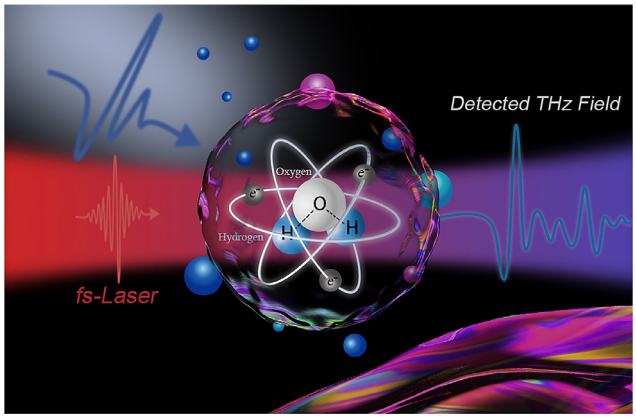

Fig. 3. Schematic of the water-based coherent detection. Low-energy femtosecond laser pulses and THz pulses are collinearly focused onto a free-flowing water film. The interference signal of the THz-induced second harmonic and a control second harmonic is measured to extract the temporal waveform of THz waves.

4. Coherent detection by free-flowing liquid targets

Liquids offer higher molecular density and nonlinearity compared to gases, which results in liquid plasmas having higher concentrations of free electrons and lower ionization thresholds [87,88]. In contrast to solid media, liquids exhibit fluidity, comparable molecular density, higher damage thresholds, and self-repaired capabilities. The potential of using liquids for coherent THz wave detection has been a focused research in the THz field. Therefore, exploring the interaction between lasers and liquid media and developing new technologies for THz wave generation and detection are of significant importance. In 2017, researchers reported on THz wave generation from liquid plasma, opening new avenues for the development of THz-related devices that utilize liquid media [89,90]. In a study conducted in 2020, bipolar birefringence signals induced by THz fields were measured in a free-flowing water film [91], providing insights into the ultrafast intermolecular hydrogen bonding dynamics in water. This highlighted potential advantages of using liquid media for THz applications.

In 2022, Ref. [92] demonstrated the coherent detection of broadband THz pulses for the first time using liquid water, which is illustrated in Fig. 3. In addition, they extended water to other liquids, such as aqueous salt solutions and ethanol. The ethanol- and solution-based coherent detection scheme further improved the detection sensitivity and obtained the nonlinear refractive index proportional relationship of different solutions in the THz band. The liquid-based coherent detection (LBCD) broadened the variety of THz wave detectors and provided the possibility of revealing the molecular interaction mechanisms in a biological liquid environment.

4.1. Liquid water

When broadband THz pulses and low-energy 800 nm laser were collinearly focused onto a ~100 μm free-flowing water film, creating a water plasma. The 400 nm THz-induced second harmonic (TISH) emitted from the water plasma was measured using a PMT. A BBO crystal was positioned in the path of the 800 nm beam to generate a controlled second harmonic (CSH) beam. When CSH beam was spatiotemporally overlapped and interfered with the TISH beam, the collected signal exhibited a linear component that correlated positively with the THz field. The underlying mechanism of this process is four-wave mixing. The coherent signal S_{THz} can be expressed as:

$$S_{THz} \propto 2\mathrm{Re}\left\{ \int_{-\infty}^{+\infty} \chi^{(3)} E_{\omega}^2\left(t - t_{THz}\right) E_{CSH}^*\left(t - t_{THz}\right) E_{THz}(t)dt \right\} \tag{14}$$

where $\chi^{(3)}$ is the third-order nonlinear coefficient of water plasma, $E_\omega(t)$ represents the electric field of the fundamental frequency laser, $E_{CSH}(t)$ represents the electric field of CSH. This method simultaneously measures the amplitude and phase of the THz field. The time-resolved waveform of the THz field with the frequency range of 0.1–18 THz was successfully achieved.

The scheme is sensitive to THz wave polarization, which was demonstrated by the dependency of the TISH energy and interference signals on the relative polarization angle θ between the fundamental frequency laser and THz field. The laser was vertically polarized and the THz polarization was rotated. The vertical component of TISH energy corresponding to $\chi^{(3)}_{yyyy}$ follows $cos^2\theta$ and the horizontal component of the TISH energy corresponding to $\chi^{(3)}_{xxyy} \approx \frac{1}{3}\chi^{(3)}_{yyyy}$ follows $sin^2\theta$ without the CSH beam imposed on the probe beam. The interference signal follows $cos\theta$ when the CSH beam was applied to ensure coherent detection and its polarization was vertical. The results indicate that the scheme can provide polarization-sensitive detection and the two orthogonal components of the THz field can be time resolved by properly rotating the polarization of the laser.

Water-based detection was well implemented with significantly lower laser energy (a few μJs) compared to air-based scheme while achieving sensitivity that is one order of magnitude higher under comparable conditions. This makes THz wave detection more achievable owing to the low laser energy requirement. Hence, our scheme is favorable for situations in the absence of sufficiently high laser energy, particularly when the laser beam needs to propagate a long distance to interact with the THz field and the beam energy is significantly depleted along the optical path.

4.2. Aqueous salt solutions

Significant variations in physicochemical properties, such as viscosity, melting point, and boiling point, distinguish various types of salt solutions from pure water. Several techniques including THz spectroscopy [93,94], ultrafast infrared spectroscopy [95,96], low-frequency Raman spectroscopy [97,98], and THz Kerr effect spectroscopy [99-101] have been utilized to investigate properties of nonlinear susceptibility and refractive index in pure water or related materials. Due to the complex components and strong absorption of aqueous salt solutions, systematically studied have not yet been conducted in the THz region. Previous spectroscopic methods have inevitable limitations. The water-based detection method can be extended to aqueous salt solutions and the detection sensitivity can be significantly enhanced owing to the typically higher $\chi^{(3)}$ of aqueous salt solutions.

In 2022, Ref. [102] demonstrated the applicability of water-based detection methods to aqueous salt solutions (cesium iodide, lithium iodide, sodium iodide, and potassium iodide). All experiments were performed under the same conditions. The results revealed that, at equivalent concentrations, the detection sensitivity of iodine ion solutions exceeded those of bromide and chloride ion solutions, with all salt solutions demonstrating greater sensitivity than pure water. The refractive index and, consequently, the detection signal strength of these solutions are directly proportional to both the refractive index and the concentration of the solid salts, showing a quadratic relationship. As the concentration of the solution increases, so does the detected signal strength, due to the corresponding increase in the refractive index linked to higher solution concentrations.

The refractive index of the solution (η_0) is proportional to the refractive index of the solid salt (η_s) and its concentration. A rough scaling of the signal intensity and η_0 is a quadratic curve. The quadratic scaling is attributed to four-wave mixing because the signal $S_{2\omega}$ linearly depends on $\chi^{(3)}$, which is quadratically proportional to η_0, as given by:

$$S_{2\omega} \propto \chi^{(3)} \propto \eta_0^2 \tag{15}$$

With the increase in solution concentration C, the relationship between the $\chi^{(3)}$, η_0, and η_s can be obtained as

$$\chi^{(3)} \propto \eta_0^2 \propto C\eta_s^2 \tag{16}$$

The correlation of the THz detection signal with $\chi^{(3)}$ or η_0 of aqueous salt solution has been established, which can be extended to more kinds of liquids and regarded as a simple rule of thumb to assess the nonlinear susceptibility of various liquids. It provides not only a scheme to enhance the sensitivity of THz coherent detection in liquids, but also provides the possibility of revealing the crucial physicochemical properties of various liquids in the THz range. Furthermore, as the rotation and vibrational energy levels of many biomacromolecules locate in the THz range, the liquid-based THz detection technique is of great potential in measuring and even controlling the characteristics of biomacromolecular solutions.

4.3. Polar liquids

Despite the significant potential of liquid water for generating and detecting THz waves, its response to THz radiation is less pronounced than that of other polar liquids, particularly ethanol [103]. Ethanol's lower ionization energy compared to water [104,105] facilitates easier ionization, requiring less laser energy to generate liquid plasma. Additionally, ethanol has a higher $\chi^{(3)}$ than water [106], enhancing its effectiveness for THz photonics applications. Studies have shown that ethanol exhibits a stronger molecular response in the THz range than pure water [107]. Moreover, research on THz wave generation has demonstrated that ethanol can emit more intense THz waves than pure water. In 2023, researchers confirmed the utility of ethanol as an effective medium for coherent THz wave detection [108], highlighting its advantages over water in this application.

By employing ethanol for THz pulse detection, the detected signals indicated that ethanol provided superior measurements compared to pure water. Furthermore, the time-domain waveform of ethanol maintained a favorable SNR even at detection energies as low as 5 μJ, opening new avenues for research into THz wave coherent detection at low laser energies. Building on these findings and theoretical analyses of coherent detection using pure water and ethanol, additional studies were conducted on THz signals detected in ethanol-water mixtures of various concentrations. The findings showed that the signal amplitude of the ethanol-water mixtures increased with the concentration of ethanol. This suggests that the time evolution curve of the coherent detection of the mixture may represent a linear superposition of the coherent detection signals from pure water and pure ethanol. This observation implies that the contribution to coherent detection is influenced by the number of ethanol and water molecules on a sub-picosecond timescale, indicating the independence of the intermolecular vibration modes within the mixtures. However, this linear superposition deviated from the measurement data when the timescale exceeded a few picoseconds, suggesting that the complex interactions among the molecular structures of the mixtures warrant further in-depth experiments for a comprehensive analysis.

Liquid-based detection scheme could potentially be applied to other similar polar liquids, such as methanol and acetone. Additionally, nonpolar liquid nitrogen has been demonstrated as a THz source. The feasibility of using other nonpolar liquids, such as liquid nitrogen and carbon disulfide, for THz wave detection remains an area for future research. Notably, although the generation and detection of THz waves in plasma channels can be analyzed in more detail in the semiclassical plasma photocurrent model, weak plasma can usually be described non-quantitatively by third-order optical rectification. This approximate nonlinear model is important for developing the water and air plasmas into convenient and flexible THz wave generators and detectors.

Table 2
Comparison of THz wave detection methods.

	PCA [19]	EOS [53]	ABCD/OBCD [62,63]	THz-REEF [79]	TEA [86]	LBCD [92]
Maximum bandwidth (THz)	100	20	40/200	10	4	18
Required laser energy	Low	Low	High	High	High	Moderate
Sensitivity	High	High	Low	Low	Low	Moderate
Damage threshold	Low	Low	High	High	High	High
Long-distance capability	N	N	N	Y	Y	N
Omnidirectional collection feasibility	N	N	N	Y	Y	N

5. Discussions and perspectives

As the earliest coherent THz wave detection technique, solid-based detection method has a broad bandwidth and high signal-to-noise ratio. However, the detector is fragile after complicated fabrication and usually could not tolerate high power laser irradiation. The gas detection methods solve the problem of low damage threshold and achieve long-distance coherent detection of THz waves. However, due to the low density of gas molecules, high-energy lasers are necessary. The liquid detection method features low required laser energy and moderate molecular density, affording a highly sensitive detection. However, due to the greater dispersion of liquids at optical wavelengths and absorption at THz frequencies, its detection bandwidth and signal-to-noise ratio are somewhat limited compared to the other two methods. As a new coherent detection technology for THz waves, liquid methods show great development potential and offer promising application prospects. Table 2 compares the detection bandwidth, long-distance transmission capability, omnidirectional collection feasibility for various solid, gas, and liquid-based detection methods, highlighting their respective advantages and disadvantages.

The development of THz wave coherent detection is of great significance in the research of THz spectroscopy and imaging technology, which benefit the fields of material analysis, biological research, and nondestructive testing. Ultrafast spectroscopy with time resolution can study the internal electronic motion of semiconductors, such as collisions and scattering between electrons and phonons, and electron migration effects. THz spectroscopy technology can be used to obtain protein fingerprints, label-free measurement of molecular reactions, label-free biochip readout, and detection of conformational changes that occur in biomolecules during their physiological functions. THz imaging can be used to monitor, detect, and identify explosives, biochemical warfare agents, and viruses in homeland security. With the advent of various intense THz sources, the interaction between THz waves and matter has become more pronounced, enabling detailed observation of biomolecular activities at the microscopic level and furthering exploration into the nonlinear properties of materials in the THz range.

Consequently, enhancing THz wave detection technology remains a pivotal focus of research. Solids, gases, and liquids have been demonstrated as materials for coherent THz wave detection. Despite significant advancements in this field over recent decades, this review captures only a limited scope of the developments. Current challenges include the limited detection bandwidth and vulnerability to damage from dielectric materials in solid-state methods, the requirement for high-energy detection light in gas methods, and the low detection sensitivity in liquid methods. Potential solutions may involve the use of solid materials that possess higher damage thresholds and improved EO coefficients, or liquids characterized by reduced absorption and increased third-order nonlinearity. It is anticipated that future breakthroughs in THz wave detection technology will reveal more compelling discoveries and significantly advance the fundamental research and applications.

Declaration of competing interest

The authors declare that they have no conflicts of interest in this work.

Acknowledgments

This work was supported by grants from the National Natural Science Foundation of China (12074272), the R&D Program of Beijing Municipal Education Commission (KZ20231002825), and the Youth Beijing Scholar Program administered by the Beijing Government.

References

[1] K.L. Chen, C.J. Ruan, F.Y. Zhan, et al., Ultra-sensitive terahertz metamaterials biosensor based on luxuriant gaps structure, iScience 26 (2023) 105781.
[2] O.P. Cherkasova, D.S. Serdyukov, A.S. Ratushnyak, et al., Effects of terahertz radiation on living cells: A review, Opt. Spectrosc. 128 (2020) 855–866.
[3] A.M. Askar, M. Saeed, A. Hamed, et al., Thickness-modulated lateral MoS_2 diodes with sub-terahertz cutoff frequency, Nanoscale 13 (2021) 8940–8947.
[4] R.Y. Zhou, C. Wang, W.D. Xu, et al., Biological applications of terahertz technology based on nanomaterials and nanostructures, Nanoscale 11 (2019) 3445–3457.
[5] G. Saavedra, M.M. Tan, J. D, Elson, et al., Experimental analysis of nonlinear impairments in fibre optic transmission systems up to 7.3 THz, J. Lightwave Technol. 35 (2019) 4809–4816.
[6] H.J. Wan, N. Liu, J. Tang, et al., Substrate-independent $Ti_3C_2T_x$ MXene waterborne paint for terahertz absorption and shielding, ACS Nano 15 (2021) 13646–13652.
[7] J. Dash, S. Ray, N. Devi, et al., Fine-tuning of terahertz resonances in hydrogen-bonded organic molecular complexes, J. Mol. Struct. 1184 (2019) 495–502.
[8] A.Y. Pawar, D.D. Sonawane, K.B. Erande, et al., Terahertz technology and its applications, Drug Invent. Today 5 (2013) 157–163.
[9] P.C. Upadhya, Y.C. Shen, A.G. Davies, et al., Terahertz time-domain spectroscopy of glucose and uric acid, J. Biol. Phys. 29 (2003) 117–121.
[10] K. Shiraga, Y. Ogawa, N. Kondo, et al., Evaluation of the hydration state of saccharides using terahertz time-domain attenuated total reflection spectroscopy, Food Chem. 140 (2013) 315–320.
[11] D.B. Hou, X. Li, J.H. Cai, et al., Terahertz spectroscopic investigation of human gastric normal and tumor tissues, Phys. Med. Biol. 59 (2014) 5423–5440.
[12] V.L. Vaks, A.V. Semenova, Yu.S. Guseva, et al., Phenomenological model and experimental study of DNA absorption spectra in THz range, Opt. Quant. Electron. 49 (2017) 193.
[13] G.Z. Liu, C. Chang, Z. Qiao, et al., Myelin sheath as a dielectric waveguide for signal propagation in the mid-Infrared to terahertz spectral range, Adv. Funct. Mater. 29 (2019) 1807862.
[14] K.J. Wu, C.H. Qi, Z. Zhu, et al., Terahertz wave accelerates DNA unwinding: A molecular dynamics simulation study, J. phys. Chem. Lett. 11 (2020) 7002–7008.
[15] Y.M. Li, C. Chang, Z. Zhu, et al., Terahertz wave enhances permeability of the voltage-gated calcium channel, J. Am. Chem. Soc. 143 (2021) 4311–4318.
[16] J.X. Zhang, Y. He, S.S. Liang, et al., Non-invasive, opsin-free mid-infrared modulation activates cortical neurons and accelerates associative learning, Nat. Commun. 12 (2021) 2730.
[17] C.H. Brodie, I. Spotts, Reguigui, et al., Comprehensive study of 3D printing materials over the terahertz regime: Absorption coefficient and refractive index characterizations, Opt. Mat. Express 12 (2022) 3379–3402.
[18] H. Kim, C. Kang, D. Jang, et al., Ionizing terahertz waves with 260 MV/cm from scalable optical rectification, Light. Sci. Appl. 13 (2024) 118.
[19] H. Shimosato, M. Ashida, T. Itoh, et al., in: S. Watanabe, K. Midorikawa (Eds.), Ultrabroadband detection of terahertz radiation from 0.1 to 100 THz with photoconductive antenna, 132, Springer, New York, 2007, pp. 317–323.
[20] P.R. Smith, D.H. Auston, M.C. Nuss, Subpicosecond photoconducting dipole antennas, IEEE J. Quantum Electron. 24 (1988) 255–260.

[21] Q. Wu, X.-C. Zhang, Free-space electro-optic sampling of terahertz beams, Appl. Phys. Lett. 67 (1995) 3523–3525.
[22] C. Fattinger, D.R. Grischkowsky, Terahertz beams, Appl. Phys. Lett. 54 (1989) 490–492.
[23] S. Kono, M. Tani, K. Sakai, Ultrabroadband photoconductive detection: Comparison with free-space electro-optic sampling, Appl. Phys. Lett. 79 (2001) 898–900.
[24] J. Zhang, Y. Hong, S.L. Braunstein, et al., Terahertz pulse generation and detection with LT-GaAs photoconductive antenna, Optoelectronics 151 (2004) 98–101.
[25] A. Singh, S. Pal, H. Surdi, et al., Carbon irradiated semi insulating GaAs for photoconductive terahertz pulse detection, Opt. Express 23 (2015) 006656.
[26] L.C. Paul, M.M. Islam, Proposal of wide bandwidth and very miniaturized having dimen-sion of μm range slotted patch THz microstrip an-tenna using PBG substrate and DGS, in: 2017 20th International Conference of Computer and Information Technology (ICCIT), 2017, pp. 1–6.
[27] L. Saurabh, A. Bhatnagar, S. Kumar, Design and performance analysis of bow-tiephotoconductive antenna for THz application, in: 2017 International Conference on Intelligent Computing and Control (12C2), 2017, pp. 1–3.
[28] J.T. Zhang, M.G. Tuo, M. Liang, et al., Terahertz emission properties of butterfly--shaped photoconductive antennas based on LT-GaAs and SI-GaAs substrates, in: 39th International Conference on Infrared, Millimeter, and Terahertz waves (IRMMW-THz), 2014, pp. 1–2.
[29] X.Y. Zhang, C.J. Ruan, J. Dai, Study of terminal truncation on log-spiral antenna characteristics at terahertz frequency, in: Progress in Electromagnetics Research Symposium-Fall (PIERS-FALL), 2017, pp. 1445–1448.
[30] C.W. Berry, N. Wang, M.R. Hashemi, et al., Significant performance enhancement in photoconductive terahertz optoelectronics by incorporating plasmonic contact electrodes, Nat. Commun. 4 (2013) 1622.
[31] N.T. Yardimci, S.H. Yang, C.W. Berry, et al., High-Power Terahertz Generation Using Large-Area Plasmonic Photoconductive Emitters, IEEE T. THz Sci. Technol. 5 (2015) 223–229.
[32] A. Jooshesh, L. Smith, M. Masnadi-Shirazi, et al., Nanoplasmonics enhanced terahertz sources, Opt. Express 22 (2014) 27992–28001.
[33] S.G. Park, K.H. Jin, M. Yi, et al., Enhancement of Terahertz Pulse Emission by Optical Nanoantenna, ACS Nano 6 (2012) 2026–2031.
[34] N.T. Yardimci, D. Turan, M. Jarrahi, Efficient photoconductive terahertz detection through photon trapping in plasmonic nanocavities, APL Photonics 6 (2021) 080802.
[35] M. Schall, M. Walther, P.U. Jepsen, Fundamental and second-order phonon processes in CdTe and ZnTe, Phys. Rev. B 64 (2001) 094301.
[36] Q. Wu, X.-C. Zhang, 7 terahertz broadband GaP electro-optic sensor, Appl. Phys. Lett. 70 (1997) 1784–1786.
[37] M. Tani, K. Horita, T. Kinoshita, et al., Efficient electro-optic sampling detection of terahertz radiation via Cherenkov phase matching, Opt. Express 19 (2011) 19901–19906.
[38] E.A. Mashkovich, A.I. Shugurov, S. Ozawa, et al., Noncollinear Electro-Optic Sampling of Terahertz Waves in a Thick GaAs Crystal, IEEE T. THz Sci. Technol. 5 (2015) 732–736.
[39] K. Liu, J.Z. Xu, X.-C. Zhang, GaSe crystals for broadband terahertz wave detection, Appl. Phys. Lett. 85 (2004) 863–865.
[40] R. Huber, A. Brodschelm, F. Tauser, et al., Generation and field-resolved detection of femtosecond electromagnetic pulses tunable up to 41 THz, Appl. Phys. Lett. 76 (2000) 3191–3193.
[41] M. Porer, J.-M. Ménard, R. Huber, Shot noise reduced terahertz detection via spectrally postfiltered electro-optic sampling, Opt. Lett. 39 (2014) 2435–2438.
[42] M. Knorr, J. Raab, M. Tauer, et al., Phase-locked multi-terahertz electric fields exceeding 13 MV/cm at a 190 kHz repetition rate, Opt. Lett. 42 (2017) 4367–4370.
[43] M. Savoini, L. Huber, H. Cuppen, et al., THz Generation and Detection by Fluorenone Based Organic Crystals, ACS Photonics 5 (2018) 671–677.
[44] I.E. Ilyakov, G.K. Kitaeva, B.V. Shishkin, et al., The use of DSTMS crystal for broadband terahertz electro-optic sampling based on laser pulse amplitude changes, Laser Phys. Lett. 15 (2018) 125401.
[45] W. Qiao, D. Stephan, M. Hasselbeck, et al., Low-temperature THz tme domain waveguide spectrometer with butt-coupled emitter and detector cystal, Opt. Express 20 (2012) 19769–19777.
[46] M. Schall, P.U. Jepsen, Freeze-out of difference-phonon modes in ZnTe and its aplication in detection of THz pulses, Appl. Phys. Lett. 77 (2000) 2801–2803.
[47] J.A. Fülöp, L. Pálfalvi, M.C. Hoffmann, et al., Towards generation of mJ-level utrashort THz pulses by optical rectification, Opt. Express 19 (2011) 1090–1097.
[48] J.A. Fülöp, L. Pálfalvi, S. Klingebiel, et al., Gneration of sub-mJ terahertz pulses by optical rectification, Opt. Lett. 37 (2012) 557–559.
[49] X.W. Ju, D.R. Chen, X.C. Chen, et al., Significant enhancement of THz detectivity by lowering ZnTe crystal temperature in electro-optic sampling, Opt. Mater. 91 (2019) 235–238.
[50] I. Wilke, J. Monahan, S. Toroghi, et al., Thin-film lithium niobate electro-optic terahertz wave detector, Sci. Rep. 14 (2024) 4822.
[51] M. Schall, H. Helm, S.R. Keiding, Far infrared properties of electro-optic crystals measured by THz time-domain spectroscopy, Int. J. Infrared Millimeter Waves 20 (1999) 595–604.
[52] M. Jazbinsek, U. Puc, A. Abina, et al., Organic crystals for THz photonics, Appl. Sci. 9 (2019) 882.
[53] U. Puc, T. Bach, P. Günter, et al., Ultra-broadband and high-dynamic-range THz time-domain spectroscopy system based on organic crystal emitter and detector in transmission and reflection geometry, Adv. Photonics Res. 2 (2021) 2000098.
[54] M. Shalini, M.G. Madhan, Photoconductive bowtie dipole antenna incorporating photonic crystal substrate for Terahertz radiation, Opt. Commun. 517 (2022) 128327.
[55] P.A. Obraztsov, V.V. Bulgakova, P.A. Chizhov, et al., Hybrid perovskite terahertz photoconductive antenna, Nanomaterials 11 (2021) 313.
[56] G. Sharma, K. Singh, I. Al-Naib, et al., Terahertz detection using spectral domain interferometry, Opt. Lett. 37 (2012) 4338–4340.
[57] H. Hirori, A. Doi, F. Blanchard, et al., Single-cycle terahertz pulses with amplitudes exceeding 1 MV/cm generated by optical rectification in $LiNbO_3$, Appl. Phys. Lett. 98 (2011) 091106.
[58] N. Karpowicz, X.F. Lu, X.-C. Zhang, et al., Terahertz gas photonics, J. Mod. Opt. 56 (2009) 1137–1150.
[59] J.M. Dai, X. Xie, X.-C. Zhang, Detection of broadband terahertz waves with a laser-induced plasma in gases, Phys. Rev. Lett. 97 (2006) 103903.
[60] N. Karpowicz, J.M. Dai, X.F. Lu, et al., Coherent heterodyne time-domain spectrometry covering the entire “terahertz gap”, Appl. Phys. Lett. 92 (2008) 011131.
[61] J.M. Dai, N. Karpowicz, X.-C. Zhang, Coherent polarization control of terahertz waves generated from two-color laser-induced gas plasma, Phys. Rev. Lett. 103 (2009) 023001.
[62] I.-C. Ho, X.Y. Guo, X.-C. Zhang, Design and performance of reflective terahertz air-biased-coherent-detection for time-domain spectroscopy, Opt. Express 18 (2010) 2872–2883.
[63] E. Matsubara, M. Nagai, M. Ashida, Ultrabroadband coherent electric field from far infrared to 200 THz using air plasma induced by 10 fs pulses, Appl. Phys. Lett. 101 (2012) 011105.
[64] X. Sun, Z.H. Lyu, H.Z. Wu, et al., Broadband terahertz detection by laser plasma with balanced optical bias, Sensors 22 (2022) 7569.
[65] X.F. Lu, X.-C. Zhang, Balanced terahertz wave air-biased-coherent-detection, Appl. Phys. Lett. 98 (2011) 151111.
[66] X.F. Lu, N. Karpowicz, X.-C. Zhang, Broadband terahertz detection with selected gases, J. Opt. Soc. Am. B. 26 (2009) A66–A73.
[67] X.F. Lu, N. Karpowicz, Y.Q. Chen, et al., Systematic study of broadband terahertz gas sensor, Appl. Phys. Lett. 93 (2008) 261106.
[68] K.-Y. Kim, J.H. Glownia, A.J. Taylor, et al., High-Power Broadband Terahertz Generation via Two-Color Photoionization in Gases, IEEE J. Quantum Electron. 48 (2012) 797–805.
[69] J. Zhang, Polarization-dependent study of THz air-biased coherent detection, Opt. Lett. 39 (2014) 4096–4099.
[70] S. Mou, A. Rubano, Q.C. Yu, et al., Terahertz unipolar polarimetry by second-harmonic generation in air, Appl. Phys. Lett. 123 (2023) 071101.
[71] Z.H. Lü, D.W. Zhang, C. Meng, et al., Polarization-sensitive air-biased-coherent-detection for terahertz wave, Appl. Phys. Lett. 101 (2012) 081119.
[72] C.-Y. Li, D.V. Seletskiy, Z. Yang, et al., Broadband field-resolved terahertz detection via laser induced air plasma with controlled optical bias, Opt. Express. 23 (2015) 11436–11443.
[73] H.W. Du, J.M. Dong, Y. Liu, et al., A coherent detection technique via optically biased field for broadband terahertz radiation, Rev. Sci. Instrum. 88 (2017) 093104.
[74] Y. Yang, M. Mandehgar, D.R. Grischkowsky, et al., Broadband THz pulse transmission through the atmosphere, IEEE T. THz. Sci. Techn. 1 (2011) 264–273.
[75] J.L. Liu, X.-C. Zhang, Terahertz-radiation-enhanced emission of fluorescence from gas plasma, Phy. Rev. Lett. 103 (2009) 235002.
[76] H.L. Xu, A. Azarm, J. Bernhardt, et al., The mechanism of nitrogen fluorescence inside a femtosecond laser filament in air, Chem. Phys. 360 (2009) 171–175.
[77] A. Filin, R. Compton, D.A. Romanov, et al., Impact-Ionization Cooling in Laser-Induced Plasma Filaments, Phys. Rev. Lett. 102 (2009) 155004.
[78] B. Clough, J.L. Liu, X.-C. Zhang, “All air-plasma” terahertz spectroscopy, Opt. Lett. 36 (2011) 2399–2401.
[79] J.L. Liu, J.M. Dai, S.L. Chin, et al., Broadband terahertz wave remote sensing using coherent manipulation of fluorescence from asymmetrically ionized gases, Nat. Photon. 4 (2010) 627–631.
[80] J.L. Liu, X.-C. Zhang, Enhancement of laser-induced fluorescence by intense terahertz pulses in gases, IEEE J. Sel. Topics Quantum Electron. 17 (2011) 229–236.
[81] J.L. Liu, J.M. Dai, X.-C. Zhang, Ultrafast broadband terahertz waveform measurement utilizing ultraviolet plasma photoemission, J. Opt. Soc. Am. B. 28 (2011) 796–804.
[82] J.L. Liu, X.-C. Zhang, Plasma characterization using terahertz-wave-enhanced fluorescence, Appl. Phys. Lett. 96 (2010) 041505.
[83] H. Sobral, M. Villagrán-Muniz, R. Navarro-González, et al., Temporal evolution of the shock wave and hot core air in laser induced plasma, Appl. Phys. Lett. 77 (2000) 3158–3160.
[84] J.L. Liu, B. Clough, X.-C. Zhang, Enhancement of photoacoustic emission through terahertz-field-driven electron motions, Phys. Rev. E. 82 (2010) 066602.
[85] H.M. Dai. J. S. Liu, S.L. Wang, et al., Physical mechanism for detecting a terahertz wave from acoustic emission enhancement in a gas plasma, J. Mod. Opt. 59 (2012) 663–666.
[86] B. Clough, J.L. Liu, X.-C. Zhang, Laser-induced photoacoustics influenced by single-cycle terahertz radiation, Opt. Lett. 35 (2010) 3544–3546.
[87] S. Minardi, A. Gopal, M. Tatarakis, et al., Time-resolved refractive index and absorption mapping of light-plasma filaments in water, Opt. Lett. 33 (2008) 86–88.
[88] J. Noack, A. Vogel, Laser-induced plasma formation in water at nanosecond to femtosecond time scales: Calculation of thresholds, absorption coefficients, and energy density, IEEE J. Quant. Electron. 35 (1999) 1156–1167.
[89] I. Dey, K. Jana, V.Y. Fedorov, et al., Highly efficient broadband terahertz generation from ultrashort laser filamentation in liquids, Nat. Commun. 8 (2017) 1184.
[90] Q. Jin, Y. W. E, Williams, et al., Observation of broadband terahertz wave generation from liquid water, Appl. Phys. Lett. 111 (2017) 071103.

[91] H. Zhao, Y. Tan, L.L. Zhang, et al., Ultrafast hydrogen bond dynamics of liquid water revealed by terahertz-induced transient birefringence, Light Sci. Appl. 9 (2020) 136.
[92] Y. Tan, H. Zhao, W.M. Wang, et al., Water-based coherent detection of broadband terahertz pulses, Phys. Rev. Lett. 128 (2022) 093902.
[93] T.W. Wang, P. Klarskov, P.U. Jepsen, Ultrabroadband THz time-domain spectroscopy of a free-flowing water film, IEEE T. THz Sci. Techn. 4 (2014) 425–431.
[94] S. Funkner, G. Niehues, D.A. Schmidt, et al., Watching the low-frequency motions in aqueous salt solutions: The terahertz vibrational signatures of hydrated ions, J. Am. Chem. Soc. 134 (2012) 1030–1035.
[95] J.T. Kindt, C.A. Schmuttenmaer, Far-Infrared dielectric properties of polar liquids probed by femtosecond terahertz pulse spectroscopy, J. Phys. Chem. 100 (1996) 10373–10379.
[96] T. Dodo, M. Sugawa, E. Nonaka, et al., Absorption of far-infrared radiation by alkali halide aqueous solutions, J. Chem. Phys. 102 (1995) 6208–6211.
[97] S.E.M. Colaianni, O.F. Nielsen, Low-frequency Raman spectroscopy, J. Mol. Struct. 347 (1995) 267–283.
[98] K. Mizoguchi, Y. Hori, Y. Tominaga, Study on dynamical structure in water and heavy water by low-frequency Raman spectroscopy, J. Chem. Phys. 97 (1992) 1961–1968.
[99] M.C. Hoffmann, N.C. Brandt, H.Y. Hwang, et al., Terahertz Kerr effect, Appl. Phys. Lett. 95 (2009) 231105.
[100] H. Zhao, Y. Tan, R. Zhang, et al., Anion-water hydrogen bond vibration revealed by the terahertz Kerr effect, Opt. Lett. 46 (2021) 230–233.
[101] Y. Tan, H. Zhao, R. Zhang, et al., Ultrafast optical pulse polarization modulation based on the terahertz-induced Kerr effect in low-density polyethylene, Opt. Express 28 (2020) 35330–35338.
[102] M.H. Zhang, W. Xiao, W.M. Wang, et al., Highly sensitive detection of broadband terahertz waves using aqueous salt solutions, Opt. Express 30 (2022) 39142–39151.
[103] P. Zalden, L.W. Song, X.J. Wu, et al., Molecular polarizability anisotropy of liquid water revealed by terahertz-induced transient orientation, Nat. Commun. 9 (2018) 2142.
[104] K. Watanabe, T. Nakayama, J. Mottl, Ionization potentials of some molecules, J. Quant. Spectrosc. Radiat. Transf. 2 (1962) 369–382.
[105] H.D. Beckey, K. Levsen, F.W. Röllgen, et al., Field ionization mass spectrometry of organic compounds, Surface Sci. 70 (1978) 325–362.
[106] A.P. Gaiduk, T.A. Pham, M. Govoni, Electron affinity of liquid water, Nat. Commun. 9 (2018) 247.
[107] H. Zhao, Y. Tan, R. Zhang, et al., Molecular dynamic investigation of ethanol-water mixture by terahertz-induced Kerr effect, Opt. Express 29 (2021) 36379–36388.
[108] W. Xiao, M.H. Zhang, R. Zhang, et al., Efficient coherent detection of terahertz pulses based on ethanol, Appl. Phys. Lett. 122 (2023) 061105.

Author profile

Guoyang Wang is a Ph.D. student at the Department of Physics, Capital Normal University. He received his bachelor's degree from China University of Petroleum in 2018 and M.S. degree of Optics from Capital Normal University in 2022, Beijing, China. His research interests include the detection of terahertz waves, as well as the interaction between air/liquid plasmas, and terahertz waves.

Ruoxi Wu is a Ph.D. student at the Department of Physics, Capital Normal University. She finished her bachelor's degree from Tangshan Normal University in 2021. Her current research interests include the generation mechanism and spatial distribution of intense terahertz wave from air plasma.

Liangliang Zhang (BRID: 09753.00.21377) is currently a full professor at the Department of Physics, Capital Normal University. She has published over 180 papers in scientific journals and possessed 36 granted Chinese patents. She won the award of National Excellent Doctoral Dissertation of China and the First Prize of Scientific Research Excellence Award from the Chinese Ministry of Education. She took charge of the National Key Scientific Instrument and Equipment Development Project of China, Beijing Science Foundation for Distinguished Young Scholars, the Youth Beijing Scholar Program of the Beijing Government, etc. Her research interests include terahertz aqueous and air photonics.

X.-C. Zhang is currently the Parker Givens Chair Professor at the Institute of Optics, University of Rochester. He is a fellow of the American Association for the Advancement of Science (AAAS), the American Physical Society (APS), the Institute of Electrical and Electronics Engineers (IEEE), the Optical Society of America (Optica), and the International Society for Optical Engineering (SPIE), and is a foreign member of the Russian Academy of Sciences. He has been granted 29 US patents and has authored or co-authored >300 academic papers with H-index of 98 in google scholar. His research focuses on the generation, detection and application of free-space terahertz beams with ultrafast optics.